Final Technical Report

Award: G15AP00039

Title: Refining estimates of late Quaternary slip rate along the Central Sierra Madre fault zone, southern California

Principal Investigator:
Reed Burgette
Department of Geological Sciences
New Mexico State University
P.O. Box 30001, MSC 3AB
Las Cruces, NM 88003
telephone: (575) 646-3782
fax: (575) 646-1056
email: burgette@nmsu.edu

In collaboration with:
Kate Scharer
Earthquake Science Center
US Geological Survey
525 South Wilson Ave.
Pasadena, CA 91106
telephone: 626-583-7240
email: kscharer@usgs.gov

Graduate student researcher:
Austin Hanson

Project duration: March 1, 2015- March 1, 2017

Abstract

This project has assessed the late Quaternary slip rate of the Central Sierra Madre fault (CSMF), the longest segment of the broader Sierra Madre fault system in Southern California. At locations where isochronous fan terrace surfaces are offset by the CSMF, we used lidar topographic data, historic air photos, and field observations to refine earlier terrace surface mapping. We dated terrace surfaces at five locations with a cosmogenic ^{10}Be depth profile technique with a new analysis strategy that incorporates uncertainties in sediment density and allows use of state-of-the-art cosmogenic nuclide production rate models. We calculate dip-slip rates using observations of the deformed markers, surface ages, and other geometric parameters, with uncertainties propagated using a Monte Carlo technique. We illustrate our approach with an example from Pickens Canyon along the western CSMF. Final ages and slip rates will be determined through integrating information from complementary IRSL dating. The slip rates from this project are the first late Quaternary slip rates for the CSMF that integrate deformation across multiple fault strands with numerical ages of offset markers. These slip rates will strengthen understanding of earthquake hazards and allow us to better asssess the role of the SMF system in the broader plate boundary system.

Report

Introduction

Motivation

The Sierra Madre fault (SMF) system juxtaposes the San Gabriel Mountains against a series of basins north of the broader Los Angeles basin (Figure 1), and represents a major seismic hazard to the residents of the greater Los Angeles area (Crook et al., 1987; Dolan et al., 1995; Rubin et al., 1998). Questions remain about the spatial variation of its slip rate, and hence seismic hazard of this approximately 135 km long reverse fault system. Along strike, the Sierra Madre fault has been divided into four main segments, from east to west: the Cucamonga, Central Sierra Madre, San Fernando, and Santa Susana faults (Figure 1). The SMF system is part of the complex collage of faults in the western Transverse Ranges, and undoubtedly interacts directly or indirectly with the adjacent San Jacinto and San Andreas faults to the east and the many reverse faults throughout the LA basin and Transverse Ranges. Estimated potential earthquake magnitudes are as high as M_w = 7.6 for single ruptures on SMF segments, and up to ~ M_w = 8 in multi-fault earthquakes (Rubin et al., 1998; Field et al., 2013). This project has focused on better resolving the late Quaternary slip rate of the Central Sierra Madre fault (CSMF) to contribute to earthquake hazard assessment and to better quantify the slip rate variation along the SMF system, to aid in resolving the role of the SMF in the broader LA Basin/Transverse Ranges area.

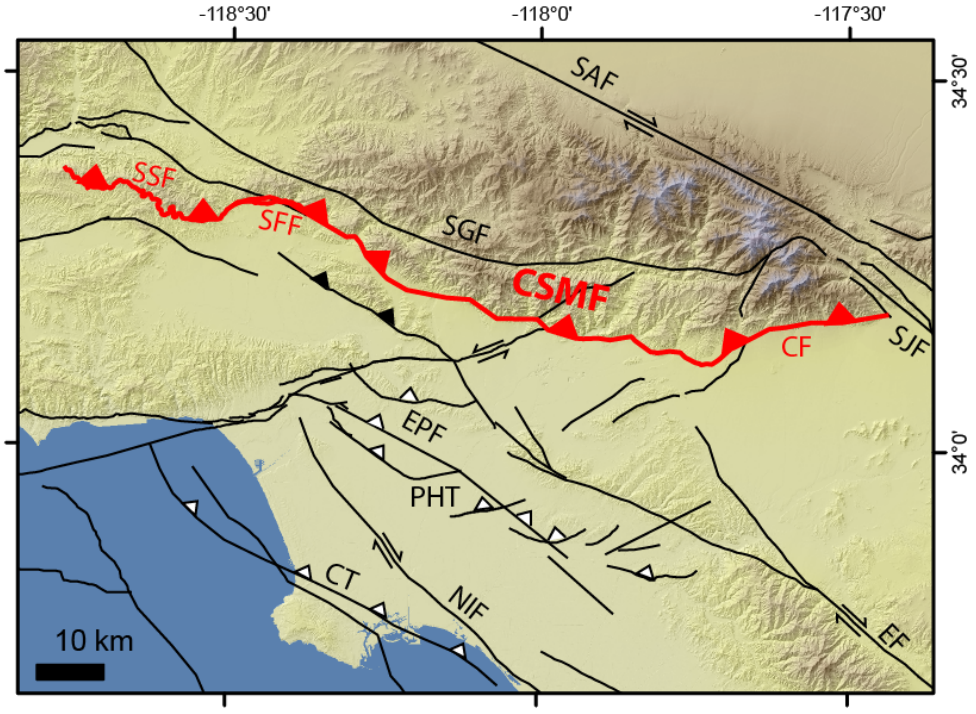

Figure 1. Context of the SMF (red), in the western Transverse Ranges. It includes the Cucamonga (CF), Central Sierra Madre (CSMF), San Fernando (SFF), and Santa Susana faults (SSF), which extend between the San Jacinto fault (SJF) and Ventura Basin (VB). Fault traces with white teeth are blind thrusts in the LA basin: EPF, Elysian Park fault; PHT, Puente Hills thrust, and CT, Compton thrust. Oblique Hollywood fault, HF. Fault traces from the SCEC Community Fault Model (Plesch et al., 2007).

Prior to this study, the slip rate along the Central Sierra Madre fault was primarily derived from trench studies. These studies are limited by both being spatially confined to one strand of a more distributed fault zone, and being temporally limited to a time span which does not average out the effects of non-uniform earthquake recurrence. This project has improved estimates of the slip rate of the Central Sierra Madre fault, which is a key component in the full SMF system.

Previous slip rate estimates for the Central Sierra Madre fault

At 85 km long, the Central Sierra Madre fault is the longest fault in the SMF system and bounds the San Gabriel basin (Yeats, 2004; Figs 2 and 3). The most extensive study of the Central Sierra Madre fault was conducted by Crook et al. (1987). They mapped Quaternary deposits along the rangefront, recognizing four ages of fan surfaces: Qal4 (oldest) to Qal1 (modern). The conventional radiocarbon dating used yielded a 2 ka age for Qal2 along the Central SMF (Crook et al., 1987). Based on correlations to dated soil chronosequences, ages of the Qal4 and Qal3 surfaces were interpreted to be ~ 300 and 10 ka, respectively. Slip rates used in the UCERF3 hazard assessment include a 4-6 m offset of a Qal2 surface exposed in a trench at Dunsmore Canyon assumed to be ~ 10 ka (Fig 2). A larger 600 m offset of Qal4 gravel at Gould Mesa from surface and borehole exposures at the Jet Propulsion Lab (JPL) site is used to yield a similar slip rate of 1.2-3 mm/yr, using an assumed age range of 200-500 ka (Crook et al., 1987; Dawson and Weldon, 2013).

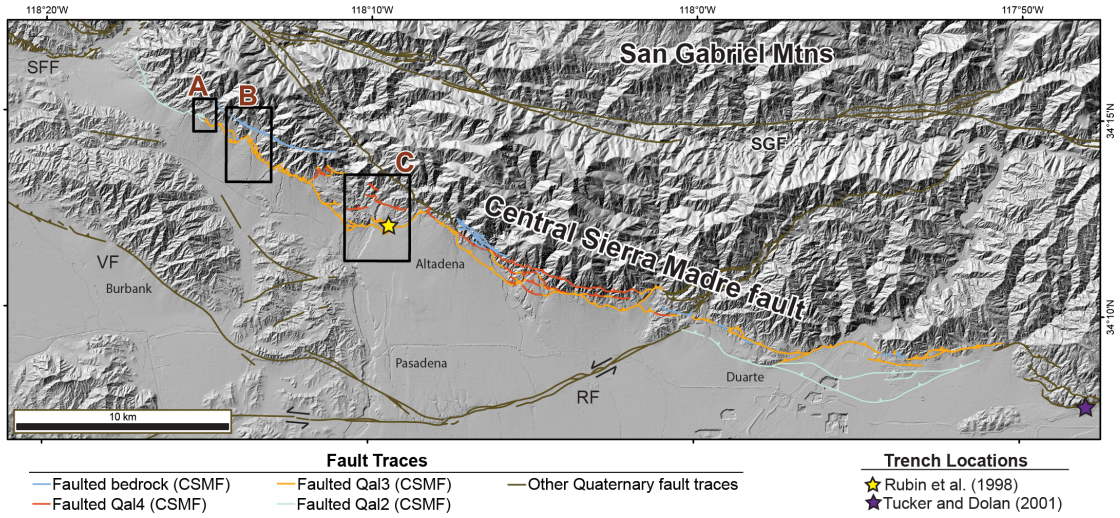

Figure 2. Map of the Central Sierra Madre fault (Burgette et al., 2016). Fault traces are from the USGS Fault and Fold Database (USGS & CGS, 2006). Faulted CSMF units are based on mapping and nomenclature of Crook et al. (1987), with Qal4 being the oldest alluvial unit. Labeled faults include: San Fernando fault (SFF), Verdugo fault (VF), Raymond fault (RF), and the San Gabriel fault (SGF). Labeled boxes show our areas of focus: A, Dunsmore Canyon; B, Pickens Canyon (the example highlighted in this report); and C, Arroyo Seco. Shaded relief basemap derived from USGS 1/3 arc second digital elevation model.

The other slip rate used in the UCERF3 assessment comes from near the eastern junction of the Central SMF with the Cucamonga fault (Fig 3). Tucker and Dolan (2001) excavated a trench across a frontal strand of the Central SMF, finding that the uppermost sediment is unfaulted, dating to 5-8 ka, based on radiocarbon on detrital charcoal. Restoration of a minimum 18 m of reverse slip since ~24 ka, yields a 0.6-0.9 mm/yr rate on the trenched strand.

Two similar rates are reported in the literature. Walls et al. (1998) summarized the Central SMF rate as 1 mm/yr. Rubin et al. (1995) trenched across a strand of the Central SMF in the Altadena area east of JPL (Fig 3) and estimated ~ 10 m of reverse slip in the last 18 ka, based on dated detrital charcoal. Some dated charcoal grains in the interpreted 18 ka layer were nearly twice as old, indicating that at least some of the organic material has a long detrital residence time. The estimated slip rate for this strand was 0.6 mm/yr (Rubin et al., 1998). Recent modeling of geodetic data yielded reverse slip rate estimates of 3.4 mm/yr (Marshall et al., 2013) and 2.7 ± 0.9 mm/yr (Daout et al., 2016). These estimates are at the upper end of geologic estimates, but lower than earlier geodetic estimates that included few of the known active faults in the area.

Methods

Quaternary Mapping

We used lidar topography with field observations to modify previous Quaternary mapping (Crook et al., 1987), with a focus on subdividing terraces by relative age at three catchments along the western CSMF. We used bare-earth lidar elevation data from the ~3 m gridded Los Angeles Regional Imagery Acquisition Consortium (LARIAC) DEM (2006) for Dunsmore and Pickens Canyons and 0.5 m gridded USGS DEM (2009) for Arroyo Seco. The classification for Quaternary alluvial units was based off of nomenclature by Crook et al. (1987), in which terraces were grouped into broad categories of Qal1, Qal2, Qal3, and Qal4, (from youngest to oldest). Alluvial surfaces were further subdivided into individual levels indicated by decimals (e.g., Qal3.2), again with lower numbers being younger in age. Relationships were determined with field observations and stratigraphic (elevation) relationships that were assessed using topographic profiles derived from lidar topography in ArcMap.

The subdivision and/or correlation of terraces is based largely on the relative topographic positions of terraces within the same catchment, which we determined by interpreting topographic profiles taken from DEMs. Cross-drainage topographic profiles were also interpreted with less certainty, but major aggradation and incisional events should be the same for adjacent drainages (e.g., Bull, 1990). We used field observations and other criteria such as continuity of deposits to ground truth to the classification of alluvial units. Our field observations of relative degree of soil development are in agreement with distinguishing characteristics originally identified by Crook et al. (1987), such as the Munsell soil color classification scheme and clast strength.

Terrace ages from TCN dating

We used ^{10}Be terrestrial cosmogenic nuclide (TCN) dating to estimate the ages of offset fan surfaces. We collected five depth profiles from the best geomorphic environments available on abandoned alluvial fan surfaces for ^{10}Be TCN dating. Sample sites were targeted to provide ages for surfaces that are preserved in both the hanging wall and footwall of major fault strands. For terraces that preserved Quaternary deformation, but were not good candidates for our dating

strategies, we dated terraces that correlate with the offset surface. Sample sites were chosen where field observations suggested minimal post-depositional modification. We excavated pits that were either dug into the interior of the fan surface, or excavated back from the edge of natural risers or other exposures to a depth of ~2 m. We collected sand to fine pebbles from 4-6 different depth intervals for each depth profile. The uppermost sample was collected below fine-grained cover sediment and the lowermost sample was collected from a depth of ~2 m below the present surface (Burgette et al., 2016).

We conducted the initial physical sample preparation at NMSU and completed physical and chemical purification and separation of Be from quartz grains at the PRIME Lab at Purdue University (modified from Kohl and Nishiizumi, 1992). Concentrations 10Be were measured on the PRIME Lab accelerator mass spectrometer, corrected for process blanks, and uncertainties were propagated following Balco (2008). We analyzed depth profiles using a new strategy that allows propagation of uncertainties due to the bulk density of the gravel. Least squares regression was used to estimate inheritance-corrected ^{10}Be concentrations and uncertainties at the upper gravel surface (modified after Selander et al., 2012). A modified procedure was used for profiles that showed evidence for sediment mixing in the upper portion of the profile to account for the effects of redistribution of the nuclide inventory with depth.

Ages and uncertainties were estimated using the CRONUSCalc online surface exposure dating calculator (Marrero et al., 2016). This enables use of newly calibrated production rates (Borchers et al., 2016), and we used the time-dependent scaling scheme of Lifton et al. (2014) to determine model ages for the terraces. The observed modern thickness of fine-grained cover sediment is input as a mass-depth above the upper gravel surface. Assumption of the present cover sediment thickness reduces the time-averaged production rate, which makes the age estimate a maximum in the case of progressive aggradation. However, this shielding effect may be counteracted by some small amount of erosion. Final estimates of terrace ages used for slip rates in this project will also incorporate information from complementary IRSL analyses.

Offset estimation

We used the hanging wall and footwall surfaces of faulted fan terraces as strain markers to calculate dip-slip displacements. We exported swath topographic data from faulted alluvial fan terraces from ArcMap as x-y-z data into MATLAB for dip-slip displacement calculations. Swaths (~30-40 m wide) are oriented near parallel to the slope of the fan surface and are subdivided into 2 m wide subswaths. We projected the subswaths to a common line that is perpendicular to the contours of the terrace surface with specified limits of the topographic data for the hanging wall, footwall, and scarp surfaces for each subswath.

We used linear regressions of the elevation profile data to resolve normal distributions of the slopes and y-intercepts of lines fit to the hanging wall ($y_h = m_h x + b_h$) and footwall ($y_f = m_f + b_f$) surfaces. We fit a third line to the scarp surface ($y_s = m_s + b_s$), which contains all possible points of the position of the fault tip ($P(x,y)$) on the scarp surface. We used a trapezoidal distribution of $P(x,y)$ values because it has been suggested that the tip of a thrust fault is most likely to be located above the bottom third and below the bottom half of the scarp surface (Carver and McCalpin, 1996; Thompson et al., 2002).

The fault dip presents a large uncertainty in the slip rate calculations due to uncertainties in fault dip and the large sensitivity of the dip-slip to the vertical component of slip at low fault dips. We used fault dips reported by Crook et al. (1987) and from the trench of Rubin et al. (1998) to guide

limits of fault dip distributions. Depending on the range of values, we used either normal or trapezoidal probability distributions of fault dips (δ).

We used Monte Carlo error propagation following the methods of Thompson et al. (2002) to calculate 6,000 dip-slip displacement estimates for each subswath, sampling through probability distributions estimated for each of the relevant geometric parameters. With 15-20 subswaths, each swath has ~100,000 slip estimates to resolve the variability in slip.

Slip rate calculation

Slip rates are estimated from the dip-slip displacements estimated at each site and terrace ages following the Monte Carlo strategy of Thompson et al. (2002). An example follows in this report using only TCN age data. However, our final rates will incorporate the full age information we have from both the TCN dating of this project and IRSL dating enabled by a complementary SCEC-funded project. Slip rate distributions from the multiple swaths and sub-swaths at each site reflect the aleatory uncertainties from the measured components of the slip rate calculation, and encompass some of the epistemic uncertainty related to terrace ages and fault dips.

Results

We obtained slip rate estimates from three locations along the western CSMF where isochronous terrace surfaces are offset by fault scarps. We conducted some reconnaissance of the central and eastern portions of the CSMF, but our observations and the mapping of Crook et al. (1987) suggested that markers of one age were not juxtaposed across the fault zone. The richest histories of terrace development and fault offset are preserved at Pickens Canyon and Arroyo Seco (Figure 2). Here we present data from the central location, Pickens Canyon (Box B, Figure 2) to illustrate our strategy and results. We summarize major results of the TCN terrace ages enabled for this project for all three sites. Full detailed results for all three sites will be presented in Hanson (2017).

Pickens Canyon example

Pickens Canyon is in La Crescenta, CA (Figure 2), where the frontal trace of the CSMF cuts late Quaternary terrace surfaces (Figure 3). We dated a prominent Q3.2 terrace surface with a TCN depth profile, and we have additional age information from IRSL dating not discussed here. We used two swath topographic profiles to estimate dip-slip displacement, and we present an example of the slip rate calculation using the TCN age estimate.

Quaternary Mapping

The alluvial units in Pickens Canyon consist predominantly of Q3 surfaces, with lesser Q4 and Q2 units. Unit Q3.2 is ~10 m higher in elevation than the inset Q3.1 surface, as is evident along the topographic profile of C-C' (Figure 4). The CSMF locally splays into two strands at Pickens Canyon, which have produced scarps on the Q3.2 terrace surface (Figure 3). The northern fault trace, 'A', is the main late Quaternary structure at Pickens Canyon, and the southern trace, 'B' has less offset (Figure 3). Crook et al. mapped two strands of additional parallel fault to the north in the bedrock, which does not appear to offset the Quaternary deposits (Figure 3). Based on the modern topography, Q3.1 does not appear to be offset (Figure 5); however, the 1935 Fairchild airphotos (flight 3758), suggest that there was a ~1 m high scarp on Q3.1 along fault strand A

prior to more extensive development (Figure 3). The topographic expression of the scarp is more subdued in the air photos than the terrace riser between units Q3.2 and Q3.1, which is about 4 m at that location.

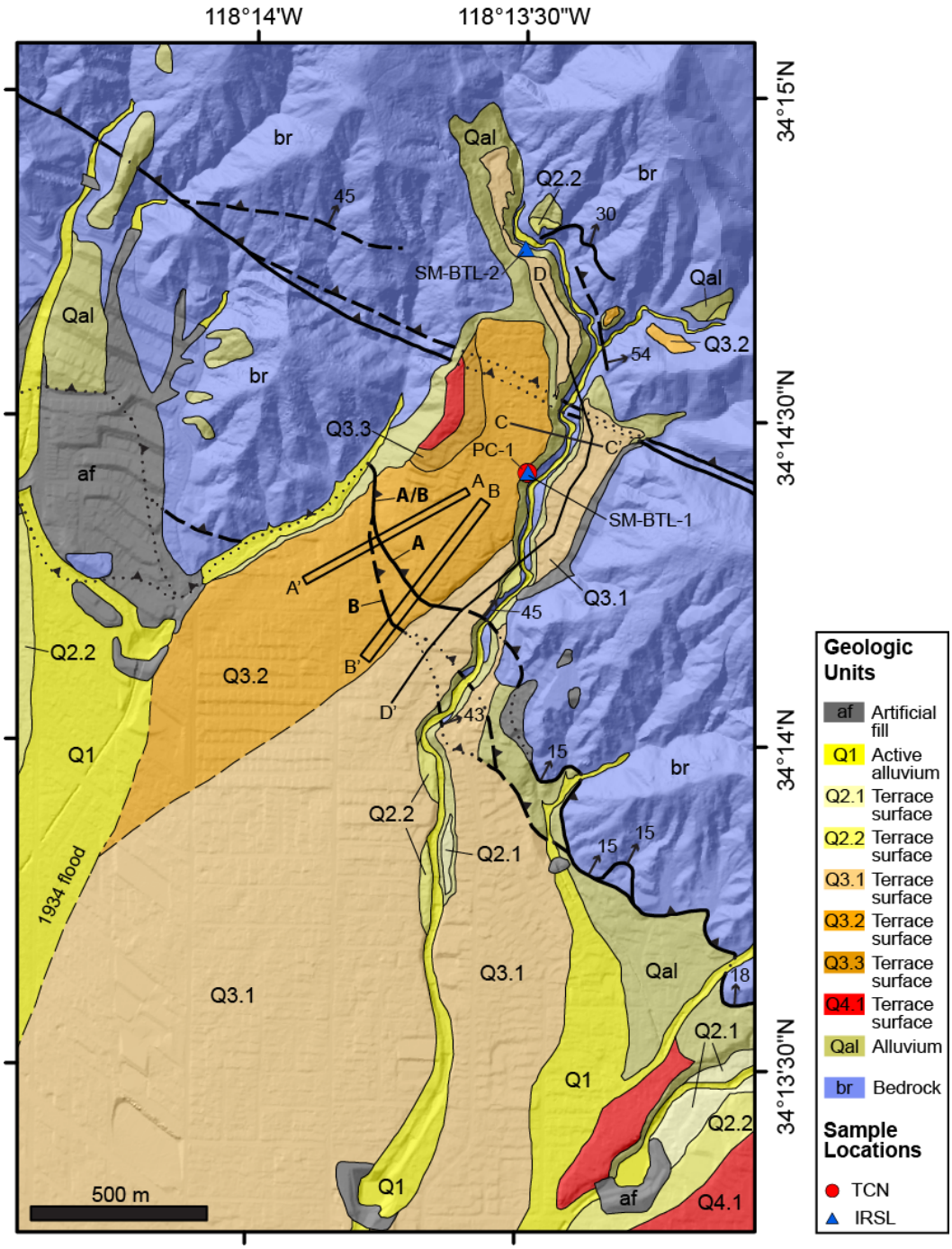

Figure 3. Geologic mapping over shaded relief (LARIAC, 2006) at Pickens Canyon (modified from Crook et al., 1987). The frontal strand of the CSMF locally splays into two strands labeled A and B, and A/B where merged. TCN and IRSL sample locations are labeled; the extent of topographic swath profiles are outlined by rectangles A-A' and B-B', and C-C', and D-D' are topographic profiles used for delineating terraces.

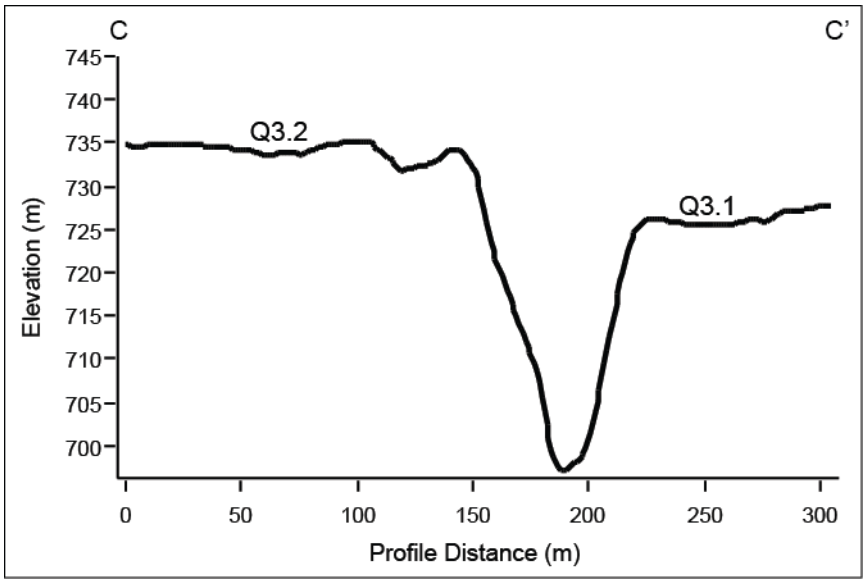

Figure 4. Topographic profile along C-C' in Pickens Canyon. The profile is oriented perpendicular to the slope of the Q3.2 and Q3.1 surfaces.

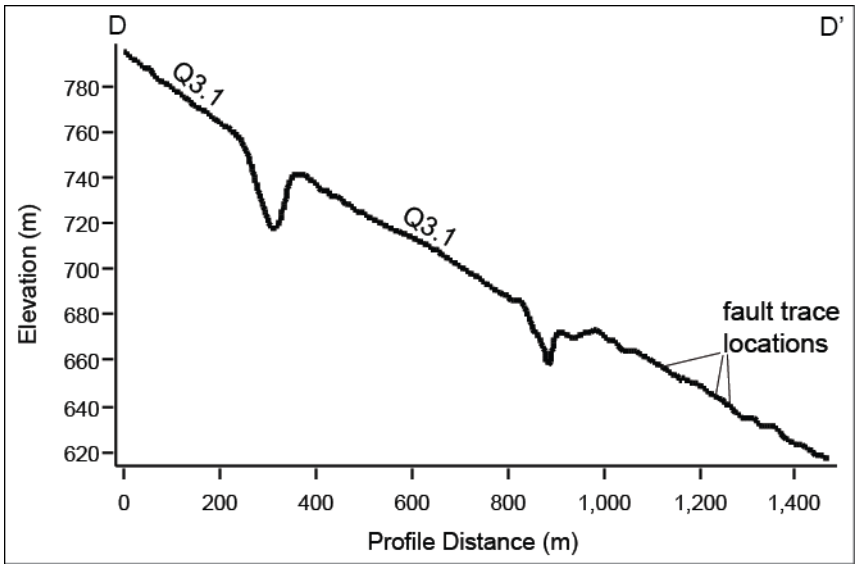

Figure 5. Topographic profile D-D' in Pickens Canyon. The profile is oriented parallel to the slopes of the three Q3.1 surface remnants. The approximate locations for the southern fault traces are shown. Crook et al. locally mapped two splays of the southern fault strand B.

Quaternary Geochronology

We collected a TCN depth profile (site PC-1) from a small, undeveloped Q3.2 terrace surface remnant (Figures 3; 6). A 0.25 m thick layer of fine-grained sediment overlies cobble gravel (Figure 6). We collected five samples of sand to fine pebbles from the gravel deposit for TCN dating. Additionally we collected light-shielded matrix material for IRSL sample SM-BTL-1 from the base of the PC-1 to test agreement between Quaternary dating techniques (Figure 6).

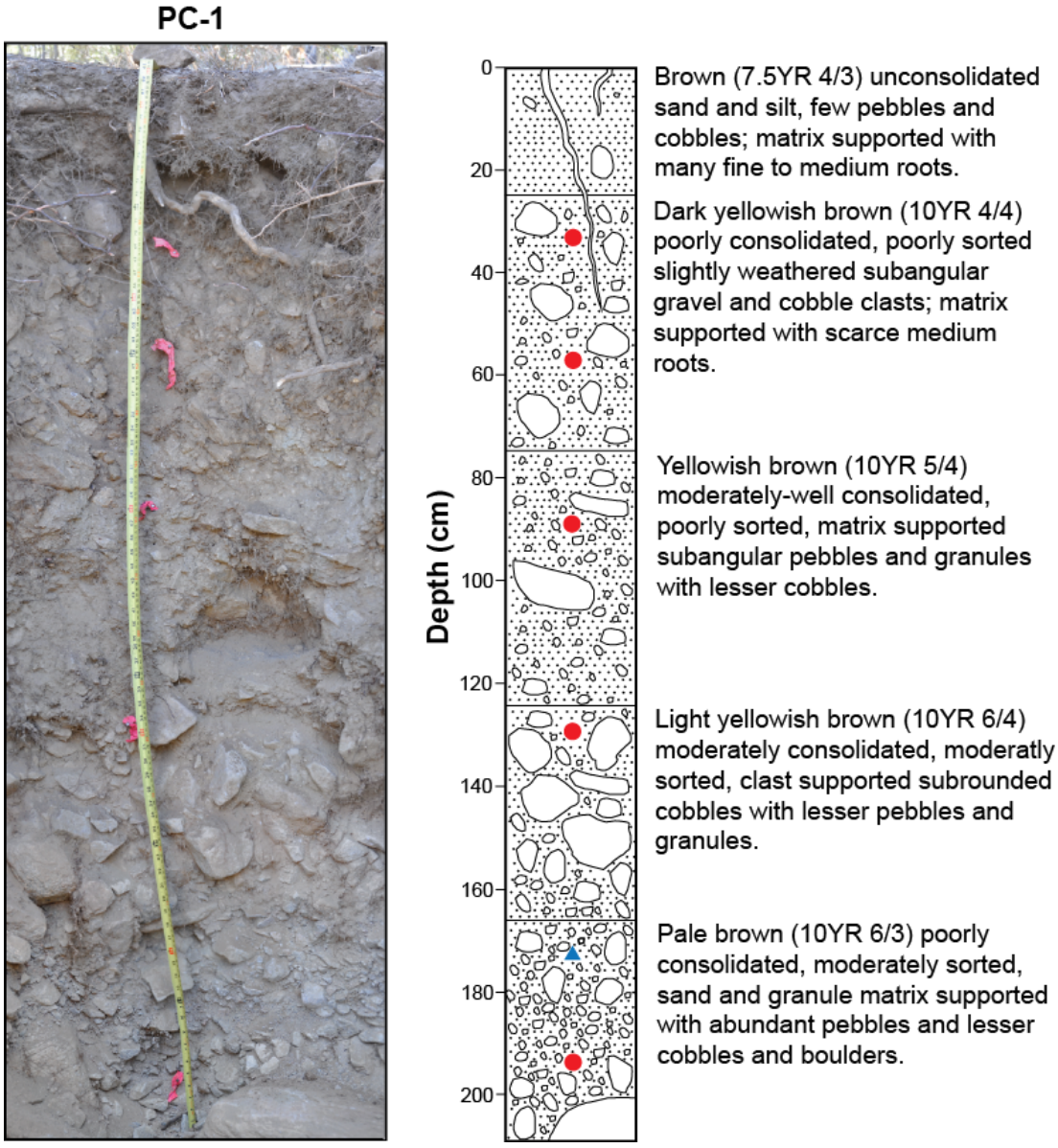

Figure 6. Photo mosaic and stratigraphic column with deposit descriptions for depth profile PC-1. The nails with pink tape in the photo represent the pre-collection approximate depths of TCN depth profile samples. The red circles in the stratigraphic column mark the mean depth of TCN depth profile samples SM-BT1-A thru SM-BT1-E, and the blue triangle marks the depth of IRSL sample SM-BTL-1.

The TCN depth profile PC-1 includes samples SM-BT1-A thru SM-BT1-E (Table 1), and we use samples SM-BT1-B thru SM-BT1-E to estimate the mean inheritance (C_i) and inheritance-corrected ^{10}Be concentrations at the top of the gravel (C_0) for five bulk density values ranging from 2.0-2.4 g/cm^3 (Figure 7). The uppermost sample, SM-BT1-A, is excluded from the C_0 estimate due to its anomalously low ^{10}Be concentration in relation to its depth. This could be due to sediment mixing associated with bioturbation within the uppermost portion of the gravel deposit. At PC-1, we estimate a C_0 of 15.70 ± 1.27 10^4 atoms/g of quartz (Table 3), where the uncertainty includes the analytical uncertainty of the depth profile data (Table 2), as well as the uncertainty of the bulk density of the gravel.

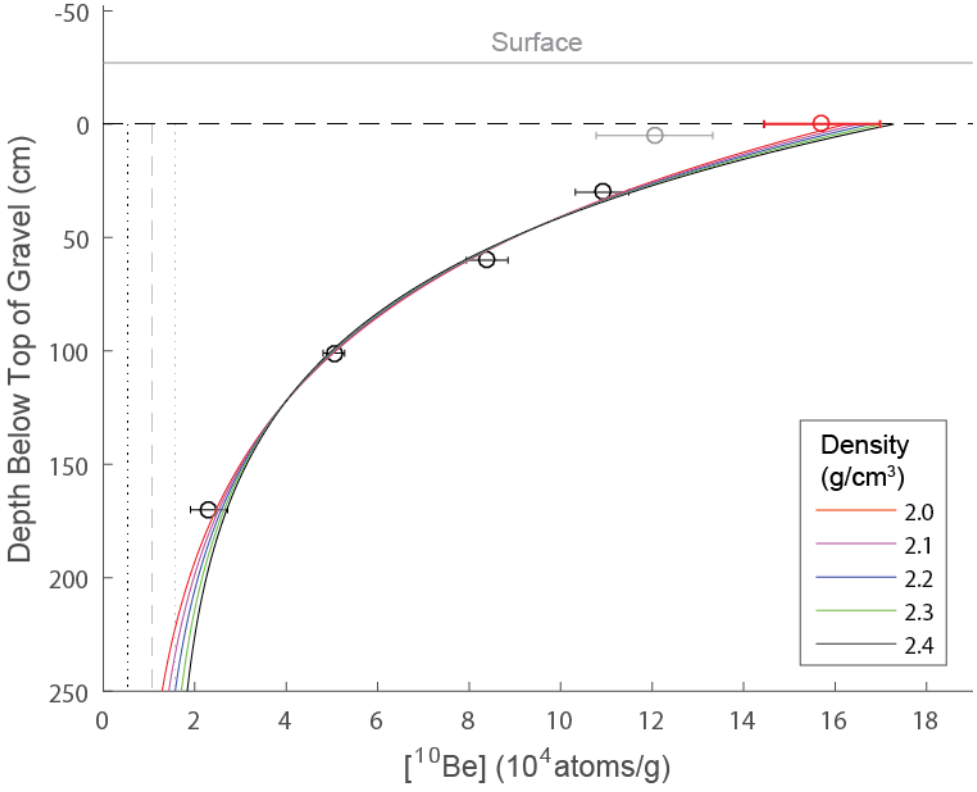

Figure 7. Inheritance (C_i) and inheritance-corrected (C_0) ^{10}Be concentration for the top of gravel of PC-1 on Q3.2 in Pickens Canyon. The mean C_i (vertical dashed line), the uncertainty of C_i (vertical dotted lines), the mean C_0 (red circle), and the uncertainty of C_0 (red error bar) are determined from the curves fit to the data (black circles) using a range of densities. The multi-colored curves are model fits to the concentration data over the considered density range. The uppermost sample (gray circle) was not included in the estimation. The surface is represented by the horizontal solid line, and the top of gravel (Figure 6) is defined by the horizontal dashed line.

Table 1
Terrestrial cosmogenic nuclide depth profile data.

Sample Site & Sample ID	Latitude (°N)	Longitude (°W)	Elevation (m)	Shielding	Depth to Top of Sample (cm)	Sampling Range (cm)	AMS Standard	[^{10}Be] (10^4atoms/ g of quartz)	[^{10}Be] Uncertainty (10^4atoms/ g of quartz)
AS-1	34.19700	118.16634	357	0.9955					
SM-FW-A					65	12	07KNSTD	3.5097	0.2407
SM-FW-B					80	14	07KNSTD	2.9994	0.2734
SM-FW-C					108	12	07KNSTD	2.3455	0.2178
SM-FW-E					162	10	07KNSTD	1.2902	0.1442
SM-FW-F					221	12	07KNSTD	0.6159	0.0777
SM-FW-G					270	10	07KNSTD	0.9111	0.2309
AS-2	34.20831	118.16433	443	0.9974					
SM-CC-A					42	11	07KNSTD	13.8930	0.7221
SM-CC-B					76	10	07KNSTD	14.2962	0.5324
SM-CC-C					123	9	07KNSTD	6.3677	0.3897
SM-CC-D					172	12	07KNSTD	3.3877	0.2999
SM-CC-E					193	16	07KNSTD	1.9186	0.1839
AS-3	34.21342	118.16747	480	0.9916					
SM-3.3-A					25	10	07KNSTD	15.3622	1.3385
SM-3.3-B					52	7	07KNSTD	11.6807	0.4712
SM-3.3-C					85	10	07KNSTD	8.0807	0.4416
SM-3.3-D					124	9	07KNSTD	4.5485	0.2818
SM-3.3-E					193	9	07KNSTD	1.9089	0.1330
AS-4	34.21369	118.16530	467	0.9677					
SM-3.1-A					55	10	07KNSTD	7.3584	0.4478
SM-3.1-B					77	10	07KNSTD	7.4913	0.3578
SM-3.1-C					114	10	07KNSTD	7.6598	0.2851
SM-3.1-D					167	11	07KNSTD	6.4177	0.5401
SM-3.1-TU					240	10	07KNSTD	1.2150	0.1043
SM-3.1-TL					350	20	07KNSTD	0.9025	0.0746
PC-1	34.24031	118.22484	719	0.9618					
SM-BT1-A					27	10	07KNSTD	12.0490	1.2753
SM-BT1-B					52	10	07KNSTD	10.9063	0.5872
SM-BT1-C					82	11	07KNSTD	8.3924	0.4552
SM-BT1-D					123	10	07KNSTD	5.0427	0.2320
SM-BT1-E					193	9	07KNSTD	2.3137	0.4044

We input the mean C_0 and uncertainty for PC-1 into the online calculator, CRONUSCalc (Marrerro et al., 2016), to estimate a model TCN surface age for Q3.2 in Pickens Canyon. For this age estimate we input the cover sediment thickness above the top of gravel as a mass depth using a density of 1.8 g/cm^3 (the density of the unconsolidated capping sediment). This yields an age estimate for PC-1 of 40.2 ± 3.9 ka, which is a maximum if the deposition of the fine-grained cover sediment occurred significantly after the abandonment of the terrace gravel. (Table 2).

Table 2
TCN model age estimates for all sites from this study following the strategy illustrated here.

Sample Site	Unit	Age (ka)	Uncertainty 1σ (ka)
AS-1	Q2.2?	21.0	1.8
AS-2	Q3.3	76.4	7.6
AS-3	Q3.3	53.0	5.5
AS-4	Q3.2	42.3	7.6
PC-1	Q3.2	40.2	3.9

Displacements and Slip rates

At Pickens Canyon, we use two topographic swath profiles to estimate the mean vertical separation ($v(x)$) of fault scarps that cut unit Q3.2 (Figure 3). The western swath, A to A' results in a $v(x)$ of 16.4 $^{+0.7}/_{-0.6}$ m (median ± 95% uncertainty) for the combined A and B strands (Figure 8). The two strands are more separated along the eastern swath profile B-B', and we estimate displacements for the two strands separately. The eastern swath, B to B' results in a $v(x)$ of 12.7 $^{+1.4}/_{-1.4}$ m for strand A, and 2.2 $^{+1.4}/_{-1.1}$ m for the southern strand B. Due to the oblique orientation of the B-B' swath with respect to the southern fault scarp (strand B), the topographic data used to fit lines to the hanging wall, scarp, and footwall surfaces were defined uniquely for each sub-swath.

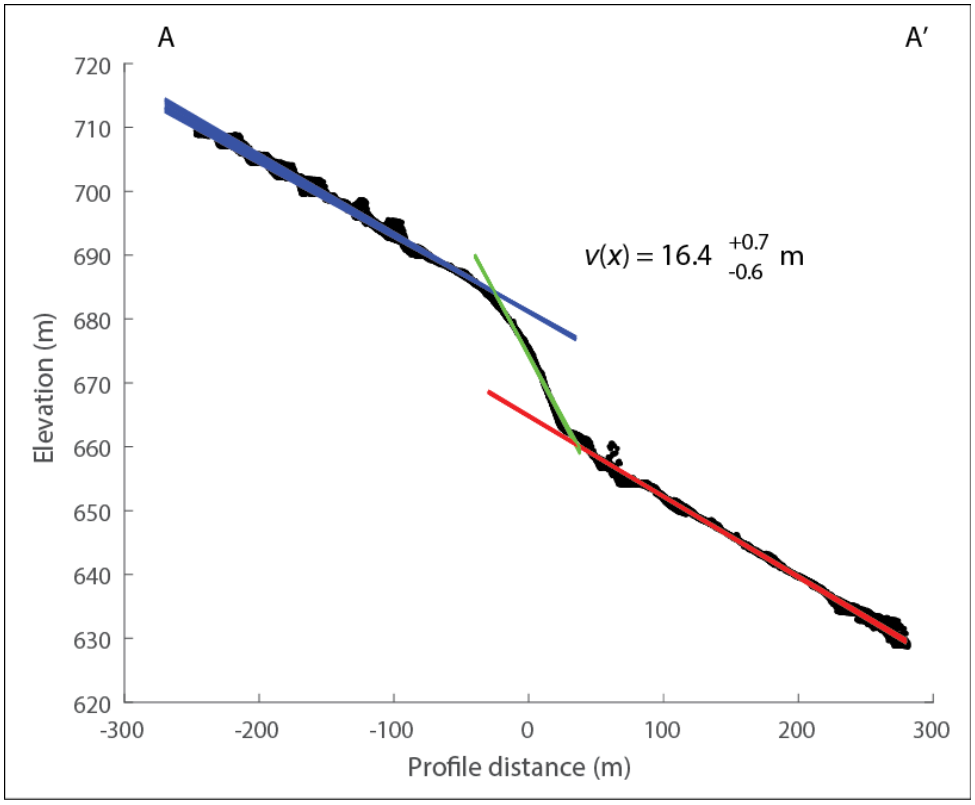

Figure 8. Topographic swath profile along A to A' at Pickens Canyon. The profile shows all of the topographic data for the 24 m wide swath zeroed on the center of the scarp. All of the hanging wall (blue), scarp (green), and footwall (red) lines fit to the 2 m wide subswaths are shown. The median vertical separation ($v(x)$) and 2σ uncertainty for the swath are derived from the subswath estimates.

We estimate the slip rate for the CSMF at Pickens Canyon using the combined slip estimates pooled from the two swaths for the two fault strands. Histograms of the relevant parameters for the slip rate for only the western profile are shown in Figure 9. Based on the fault dips reported by Crook et al. (1987) in the area of Pickens Canyon (Figure 3), we use dips of 45 and 15 degrees for the maximum and minimum values of the plateau portion of our trapezoidal fault dip distribution (Figure 9). In this example, we use our Q3.2 surface TCN age estimate of 40.2 ± 3.9

ka, assuming Gaussian uncertainty (Table 2; Figure 9E) . For the western swath along A-A', the $v(x)$ (Figures 8 and 9B) measured at all possible points, $P(x)$, (Figure, 9A), and the fault dip PDF (Figure 9C) yields a dip-slip displacement (s) of 41.5 $^{+116.9}/_{-16.4}$ m (Figure, 9D). Using the Q3.2 TCN age in Pickens Canyon (Figure 9E), we estimate a slip rate of 1.04 $^{+2.93}/_{-0.45}$ mm/yr (Figure 9F) for this location.

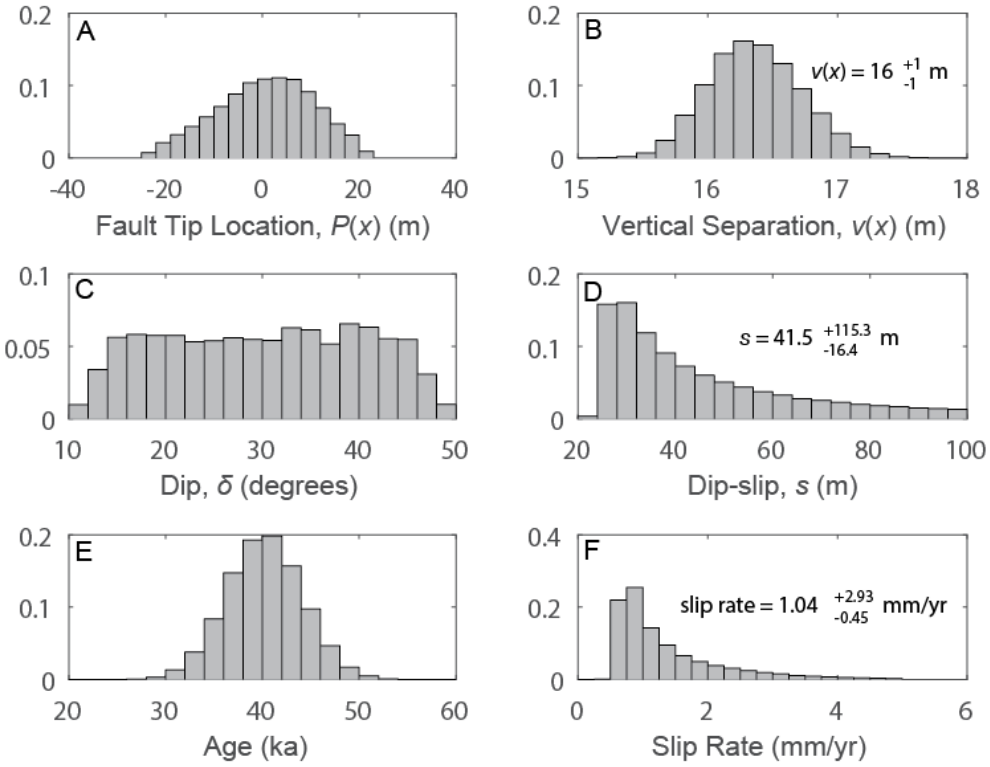

Figure 9. Histograms of parameters used to estimate slip rate of the CSMF along along swath A-A' at Pickens Canyon. Probability is represented on the y-axis for all histograms. The median estimated values and 2σ uncertainty for the vertical separation ($v(x)$), dip-slip (s), and slip rate, are reported.

The slip estimates from the eastern swath B-B' are similar to those from Figure 9 although measured along a different azimuth and across two separate fault strands. When the displacements are pooled together, the resulting slip rate estimate is 1.05 $^{+2.91}/_{-0.47}$ mm/yr (Figure 10), quite similar to the example estimate from the western swath alone (Figure 9F). Although the uncertainties are large at the 95% level reported here, the 84th percentile is ~2 mm/yr. The long right tails of the slip and slip rate distributions are largely driven by the low dip angles observed in some exposures of the CSMF.

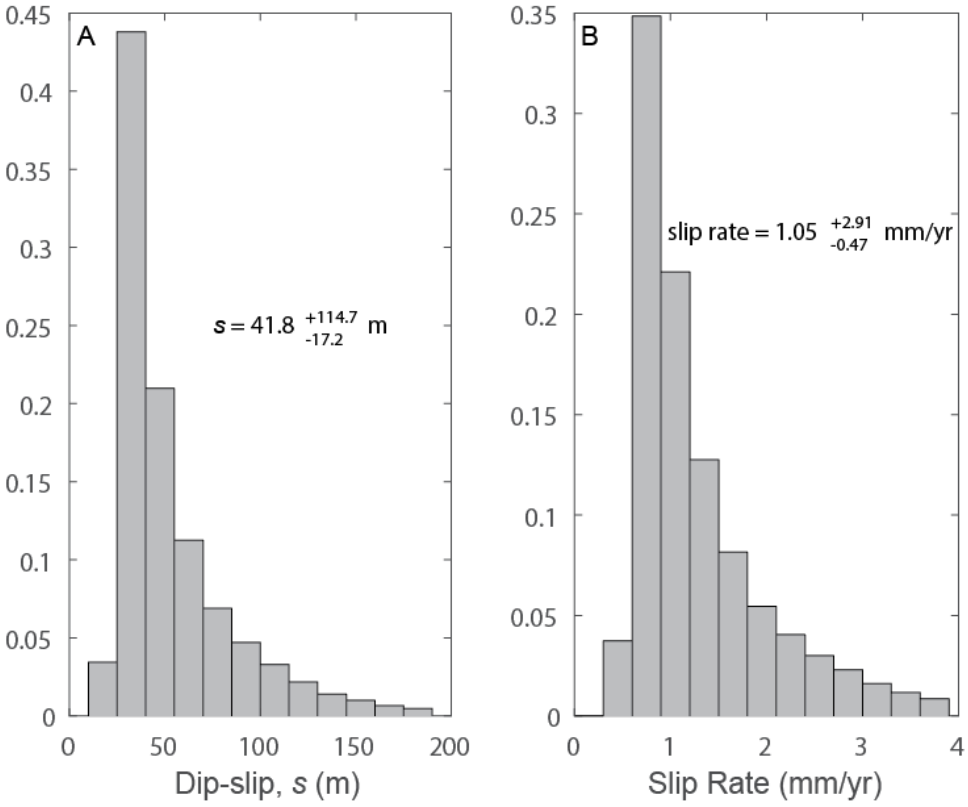

Figure 10. Composite dip-slip displacement (A), and slip rate (B) for both swaths at Pickens Canyon using the TCN age. Probability is represented on the y-axis for both plots. Note the similarities of the distributions to those of Figure 9 for the west swath only.

Conclusions and next steps

We have estimated vertical separations of terrace surfaces and associated dip-slip displacements at the most promising locations along the Central Sierra Madre fault. Terrestrial cosmogenic nuclide dating has yielded ages for the most prominent faulted terrace surface at Pickens Canyon, the example of this report, as well as four terraces in the Arroyo Seco catchment. We are estimating slip rates using displacements and ages, with uncertainties propagated from the uncertainties from the relevant input parameters. Preliminary slip rate estimates are generally consistent with the previous geologic slip rate estimates for this fault, although higher rates are permissible if the fault dip is low angle.

We are in the process of making final interpretations of how to best incoporporate the TCN ages funded by this project with information from the complementary SCEC-funded IRSL ages. Final terrace age probability distributions will be used to estimate final slip rates for all the sites of our study. We will use our results to evaluate along-strike trends in deformation rate and slip history for the CSMF and broader SMF system when integrated with prior geologic and geodetic studies. These final components will be completed for graduate student Austin Hanson's M.S. thesis which will be defended later in summer 2017. We plan to submit this work for scholarly publication soon thereafter.

Papers and presentations related to this project

Burgette, R.J., Hanson, A.M., Scharer K.M., and Midttun, N., 2016, Late Quaternary offset of alluvial fan surfaces along the Central Sierra Madre fault, Southern California, in J.P. McCalpin & C. Gruetzner (Eds.), Proceedings of the 7th International INQUA Meeting on Paleoseismology, Active Tectonics and Archeoseismology, Crestone Science Center, Crestone, CO, ISBN 978-0-9974355-2-8, p. 50-53.

Hanson, A.M., Burgette, R.J., Scharer K.M., and Midttun, N., 2016, Late Quaternary slip rates from offset alluvial fan surfaces along the Central Sierra Madre fault, southern California, SCEC Annual Meeting, Poster 096, Palm Springs, CA Sept. 11-14.

Hanson, A.M.*, Burgette, R.J., Scharer K.M., and Midttun, N., 2015, Late Quaternary Offset of Alluvial Fan Surfaces along the Central Sierra Madre Fault, Southern California, Abstract T41A-2857, presented at 2015 Fall Meeting, AGU, San Francisco, Calif., 14-18 Dec.

Hanson, A.M., Burgette, R.J., Scharer K.M., and Midttun, N., 2015, Late Quaternary Offset of Alluvial Fan Surfaces along the Central Sierra Madre Fault, Southern California, SCEC Annual Meeting, Palm Springs, CA Sept. 9-11, 2015.

References cited

Balco, G., Stone, J. O., Lifton, N. A., and Dunai, T. J. (2008). A complete and easily accessible means of calculating surface exposure ages or erosion rates from 10Be and 26Al measurements: Quaternary Geochronology v. 3, p. 174-195.

Borchers, B., Marrero, S., Balco, G., Caffee, M., Goehring, B., Lifton, N., Nishiizumi, K., Phillips, F., Schaefer, J. and Stone, J. (2016). Geological calibration of spallation production rates in the CRONUS-Earth project: Quaternary Geochronology, v. 31, p.188-198.

Bull, W.B. (1991). *Geomorphic responses to climatic change*: London, Oxford University Press, 326 p.

Carver, G. A., and McCalpin, J. P. (1996). Paleoseismology of compressional tectonic environments, *in* McCalpin, J. P., ed., *Paleoseismology*: New York-London-Toronto, Academic Press, p. 183-270.

Crook, R. Jr., Allen, C.R., Kamb, B., Payne, C.M., & Proctor, R.J. (1987). Quaternary geology and seismic hazard of the Sierra Madre and associated faults, western San Gabriel Mountains, Recent reverse faulting in the Transverse Ranges, California: US Geological Survey Professional Paper, 1339, 27-64.

Daout, S., S. Barbot, G. Peltzer, M.-P. Doin, Z. Liu, and R. Jolivet (2016), Constraining the kinematics of metropolitan Los Angeles faults with a slip-partitioning model, Geophysical Research Letters, 43, 11,192–11,201.

Dawson, T. E., & Weldon II, R. J. (2012). Appendix B: Geologic Slip-Rate Data and Geologic Deformation Model, Uniform California earthquake rupture forecast, version 3 (UCERF3)—The time-independent model. US Geological Survey Open-File Report, 1165.

Dolan, J. F., Sieh, K., Rockwell, T. K., Yeats, et al., (1995). Prospects for larger or more frequent earthquakes in the Los Angeles metropolitan region. Science, 267, 199-205.

Field, E. H., Biasi, G. P., Bird, P., Dawson, T. E., et al. (2013). Uniform California earthquake rupture forecast, version 3 (UCERF3)—The time-independent model. US Geological Survey Open-File Report, 1165, 97 p.

Hanson, A.M. (2017), Late Quaternary slip rate of the Central Sierra Madre fault, southern California, M.S. thesis, New Mexico State University, *in preparation*.

Kohl, C., Nishiizumi, K., 1992. Chemical isolation of quartz for measurement of in-situ-produced cosmogenic nuclides. Geochimica Et Cosmochimica Acta 56, 3583-3587.

Lifton, N., Sato, T., Dunai, T.J. (2014). Scaling in situ cosmogenic nuclide production rates using analytical approximations to atmospheric cosmic-ray fluxes. Earth and Planetary Science Letters 386, 149–160. doi:10.1016/j.epsl.2013.10.052

Marrero, S. M., Phillips, F. M., Borchers, B., Lifton, N., Aumer, R., & Balco, G. (2016). Cosmogenic nuclide systematics and the CRONUScalc program. Quaternary Geochronology, 31, 160-187.

Marshall, S. T., Funning, G. J., & Owen, S. E. (2013). Fault slip rates and interseismic deformation in the western Transverse Ranges, California. Journal of Geophysical Research: Solid Earth, 118(8), 4511-4534.

Plesch, A., Shaw, J. H., Benson, C., et al. (2007). Community fault model (CFM) for southern California. Bulletin of the Seismological Society of America, 97(6), 1793-1802.

Rubin, C. M., Lindvall, S. C., & Rockwell, T. K. (1998). Evidence for large earthquakes in metropolitan Los Angeles. Science, 281(5375), 398-402.

Selander, J., Oskin, M., Ormukov, C., and Abdrakhmatov, K. (2012). Inherited strike‐slip faults as an origin for basement-cored uplifts: Example of the Kungey and Zailiskey ranges, northern Tian Shan: Tectonics, v. 31, p. TC4026, doi:10.1029/2011TC003002.

Thompson, S. C., Weldon, R. J., Rubin, C. M., Abdrakhmatov, K., Molnar, P., & Berger, G. W. (2002). Late Quaternary slip rates across the central Tien Shan, Kyrgyzstan, central Asia. Journal of Geophysical Research: Solid Earth, 107(B9), 2203.

Tucker, A. Z., & Dolan, J. F. (2001). Paleoseismologic evidence for a> 8 ka age of the most recent surface rupture on the eastern Sierra Madre fault, northern Los Angeles metropolitan region, California. Bulletin of the Seismological Society of America, 91(2), 232-249.

U.S. Geological Survey and California Geological Survey (2006) Quaternary fault and fold database for the United States, accessed 1/24/2014, from USGS web site: http//earthquakes.usgs.gov/regional/qfaults/.

Walls, C., Rockwell, T., Mueller, K., Bock, Y., et al. (1998). Escape tectonics in the Los Angeles metropolitan region and implications for seismic risk. Nature, 394(6691), 356-360.